Liquid Crystals
Publication details, including instructions for authors and subscription information:
http://www.informaworld.com/smpp/title~content=t713926090

Anomalous effects in experiments on monodomain nematic and lamellar phases of the caesium pentadecafluorooctanoate(CsPFO)/water system

N. Boden[a]; G. R. Hedwig[a]; M. C. Holmes[b]; K. W. Jolley[c]; D. Parker[a]
[a] School of Chemistry, University of Leeds, England [b] Department of Physics and Astronomy, Lancashire Polytechnic, Preston, England [c] Department of Chemistry and Biochemistry, Massey University, Palmerston North, New Zealand

To cite this Article Boden, N. , Hedwig, G. R. , Holmes, M. C. , Jolley, K. W. and Parker, D.(1992) 'Anomalous effects in experiments on monodomain nematic and lamellar phases of the caesium pentadecafluorooctanoate(CsPFO)/water system', Liquid Crystals, 11: 3, 311 — 324
To link to this Article: DOI: 10.1080/02678299208028991
URL: http://dx.doi.org/10.1080/02678299208028991

LIQUID CRYSTALS, 1992, VOL. 11, NO. 3, 311–324

Anomalous effects in experiments on monodomain nematic and lamellar phases of the caesium pentadecafluorooctanoate(CsPFO)/water system

by N. BODEN*†, G. R. HEDWIG‡, M. C. HOLMES§, K. W. JOLLEY*‡ and D. PARKER†

† School of Chemistry, University of Leeds, LS2 9JT, England
‡ Department of Chemistry and Biochemistry, Massey University, Palmerston North, New Zealand
§ Department of Physics and Astronomy, Lancashire Polytechnic, Preston PR1 2TQ, England

(*Received 15 April 1991; accepted 17 August 1991*)

The effects of defects on a variety of experiments on monodomain nematic and lamellar phases of the CsPFO/water system are described. In NMR experiments the observed anomalous behaviour depends on whether the sample tube is oriented with its long axis perpendicular or parallel to the direction of the applied magnetic field. In the former case, focal domains are shown to lead to a distortion of the spectra on heating, but not on cooling the sample; whereas, in the latter case, dislocations (possibly of the edge variety) are generated on cooling and focal domains on heating. Similar defects can lead to anomalous effects in measurements of bulk properties such as the electrical conductivity, as demonstrated here. In density measurements on unoriented samples using a vibrating capillary densitometer, anomalous decreases in density are observed at the isotropic-to-nematic and nematic-to-lamellar phase transitions. These anomalies are absent in density measurements using a classical dilatometer.

1. Introduction

The phase behaviour [1–3] and structure [4–7] of the caesium pentadecafluorooctanoate(CsPFO)/water, and related systems [8–13] has attracted the attention of liquid crystal scientists in recent years. This is because it forms a discotic nematic phase N_D^+ of exceptional stability (w(CsPFO): 0·225 to 0·632; temperature: 285·3 to 351·2 K in the heavy water system; w(CsPFO): 0·235 to 0·632; temperature: 281·3 to 342·7 K in the water system [3]) and positive diamagnetic susceptibility. It lies between an isotropic solution phase I of discotic micelles, to lower concentrations/higher temperatures, and a discotic lamellar phase L_D, to higher concentrations/lower temperatures. Its positive magnetic susceptibility enables monodomain N_D^+ and L_D phases to be obtained in applied magnetic fields, providing opportunities for precise experimental studies. However, the presence of defects can give rise to anomalous effects in such experiments. Whilst the occurrence of such defects has been acknowledged on several occasions [2, 7, 13], the implications of their presence for the interpretation of experimental observations has still to be addressed. The object of this paper is to describe the nature of these defects and their dependence on the constraints of the sample container and thermal history. In particular, their impact on a variety of

* Authors for correspondence.

0267–8292/92 $3·00

experiments, including NMR, optical microscopy, electrical conductivity and density measurements, is outlined. Consideration of the nature of the defects involved, all of which have been previously characterized [14], leads to protocols for the avoidance of anomalous effects in such experiments.

2. NMR experiments

Since the nematic phase of CsPFO/^2H_2O is diamagnetically positive, the nematic director **n** undergoes spontaneous alignment along the direction of the spectrometer magnetic field **B** to give a macroscopically aligned sample. For this, and also for the macroscopically aligned L_D phase, the spectrum of the ^2H spin in labelled water molecules will be a simple doublet with separation, referred to as the quadrupole splitting, given by

$$\Delta\tilde{\nu}(\phi) = 3|\tilde{q}_{zz}|_s S P_2(\cos\phi)/2, \tag{1}$$

where the upper tilde denotes partially averaged quantities. $|\tilde{q}_{zz}|_s$ is the partially averaged component of the nuclear-quadrupole electric-field-gradient interaction tensor measured parallel to **n** in a perfectly ordered mesophase: its explicit form, discussed elsewhere [2], depends upon the size and volume fraction of the micelles. S is the second rank orientational order parameter for the orientational fluctuations of the micellar axes M(a, b, c) with respect to **n**: it is given by $\langle P_2(\cos\beta)\rangle$ where β is the angle between the symmetry axis c and **n**. ϕ is the angle between **n** and **B**.

For a homeotropic director distribution, all ϕ will be the same and each component of the doublet will be a sharp line of width determined by the spin–spin relaxation time T_2 (linewidth at half maximum height $= 1/\pi T_2$). The spectra in figure 1 show that this situation obtains in both the N_D^+ and L_D phases when a sample is cooled in an iron magnet with the axis of the cylindrical sample tube orientated perpendicular to the direction of **B**. But, on heating (from the L_D phase at 290 K), intensity corresponding to values of ϕ other than zero degrees begins to build up in the spectrum. This is most apparent in the appearance of the doublet with separation one half of that of the principle doublet corresponding to $\phi = 0°$. This arises from volume elements whose directors are orientated at $\phi = 90°$. On heating into the N_D^+ phase, the spectrum reverts to a simple doublet, indicating that the homeotropic director distribution is re-established.

The distribution of directors obtained on heating the L_D phase must arise from the presence of defects. The nature of these defects can be ascertained by observing the changes in optical texture (see figure 2) employing a corresponding thermal treatment of a sample of identical composition contained in a parallel-sided flat glass capillary cell. A homeotropic film is first obtained by cycling across the N_D^+ to L_D transition (see figure 2 (*a*)). When cooled, the homeotropic texture remains unchanged down to 295 K, just above the temperature at which crystalline surfactant begins to separate. However, on warming, the homeotropic texture is replaced by a parabolic-focal-conic texture [15] (figure 2 (*b*)). This texture is stable for periods of many hours. The growth of the parabolic-focal-conic texture is reversible: on cooling back to 295 K, the homeotropic texture is re-established. The parabolic-focal-conic texture indicates small lamellar regions arranged on a square lattice in which the lamellae have moved away from their homeotropic orientation. The parabolic-focal-conic texture relaxes to a homeotropic one on heating into the nematic phase, although the process can be slow, being governed by the rather high viscosity coefficients in the nematic phase close to T_{LN}.

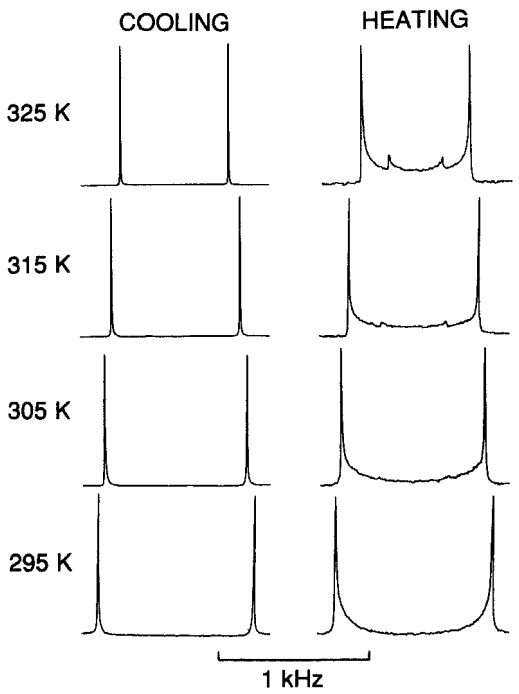

Figure 1. ^2H NMR spectra of ^2H_2O in a sample of CsPFO/^2H_2O (w=0·550) obtained at 9·21 MHz using a JEOL FX60 spectrometer with an iron magnet of flux density 1·41 T. The sample, 30 mm in length, is contained in a 5 mm o.d. cylindrical glass tube with its long axis perpendicular to the direction of the field. The rate of cooling/heating was 0·5 K/min and at any of the measured temperatures the spectra were found to be invariant over at least 24 hours. For w=0·550 the phase transition temperatures are: T_{IN} (the upper temperature limit of the isotropic-to-nematic transition)=330·64 K; T_{NI} (the lower temperature limit of the isotropic-to-nematic transition)=330·09 K; T_{NL} (the upper temperature limit of the nematic-to-lamellar transition)=325·82 K; T_{LN} (the lower temperature limit of the nematic-to-lamellar transition)=325·10 K. Temperature control was achieved using a double pass water flow system in conjunction with a Colora WK3 cryothermostat [2]. The same temperature control system was used to obtain the spectra shown in figure 6 and the conductivity measurements shown in figure 9.

The parabolic-focal-conic structure is a characteristic of liquid crystal phases having a layer-like structure and occurs when a dilative strain is present in a direction perpendicular to the layers. This strain may be realized in practice either by a mechanical movement of the container walls, as has been discussed extensively for thermotropic smectic phases [15], or by causing the layers themselves to contract within a cell of fixed width by a change in temperature, as has been demonstrated for lyotropic lamellar phases [16, 17]. The latter is the origin of the parabolic-focal-conic tructure in the CsPFO system: figure 3 illustrates how the lamellar repeat distance d decreases as the sample is heated. Raising the temperature by an amount ΔT causes the layer spacing to decrease by an amount Δd. Constrained by the cell walls, with separation a (see figure 4 (*a*)), the system experiences a stress with a concomitant strain $\sigma \approx \Delta d/d_0$, where d_0 is the value of d at the start temperature. The lamellar planes are predicted [15, 18] to buckle to relieve the stress (see figure 4 (*b*)), once a critical strain σ_c has been exceeded

$$(\Delta d/d_0)_c = \sigma_c = (2\pi/a)(k_{11}/B)^{1/2} = (2\pi\lambda/a), \quad (2)$$

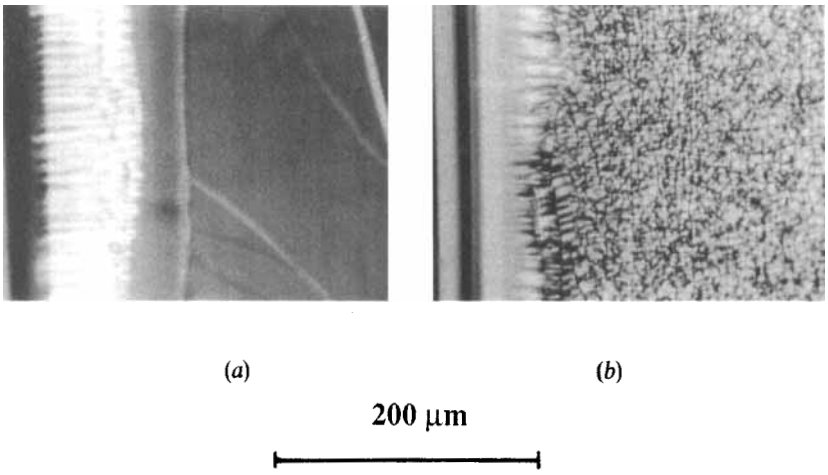

Figure 2. Photomicrographs of the lamellar phase of a sample of CsPFO/^2H_2O (w = 0·550) contained in a parallel-sided flat glass capillary cell of thickness 0·2 mm. (*a*) Shows a homeotropic sample at 295 K; the edge of the glass cell is visible as the bright, birefringent region on the left. (*b*) Shows the parabolic-focal-conic texture obtained when the sample is heated to 325 K, just below T_{LN}.

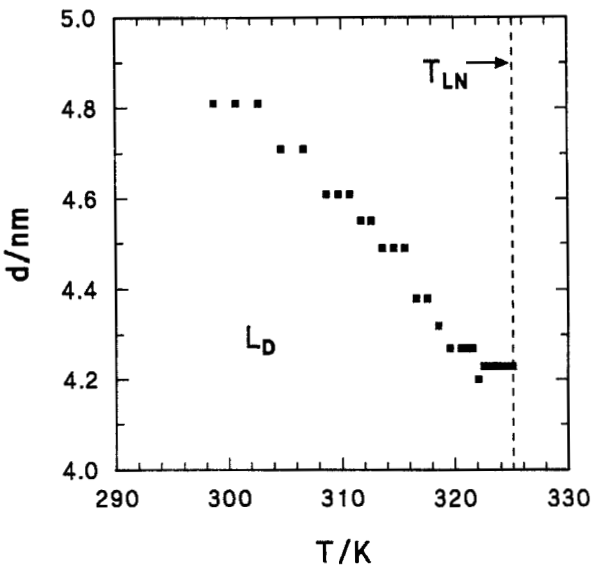

Figure 3. Lamellar repeat distance *d* as a function of temperature for CsPFO/^2H_2O (w = 0·550). The measurements represent an extension of those previously reported [5].

where k_{11} is the splay elastic constant and B is the compressional elastic constant. The periodicity of the undulations $2\pi/k$ (figure 4 (*b*)) is related to the characteristic length $\lambda\ \{=(k_{11}/B)^{1/2}\}$ by $k^2=\pi/\lambda a$. Rosenblatt *et al.* [15] have shown that as the dilative strain increases to $\sigma>1{\cdot}5\sigma_c$, there is the onset of a parabolic-focal-conic structure, represented in two dimensions in figure 4 (*c*), and having a characteristic optical texture as shown in figure 2 (*b*). By assuming that the period of this array corresponds to that of the undulation pattern seen at lower strain, the characteristic half width of the parabolae at the surface is [15]

$$R_0=\pi/k=(\pi\lambda a)^{1/2}. \tag{3}$$

From measurements of R_0 at 300 K for samples in cells of widths: 0·2, 0·1 and 0·05 mm, a mean value of 30 ± 4 nm was obtained for λ. This is about six times the layer repeat distance (see figure 3) in contrast to thermotropic smectic A phases for which λ is of the same order as d (for CBOOA at 351 K, $\lambda=2{\cdot}2$ nm [19]). This result is indicative of a relatively smaller compressional elastic constant for the lyotropic system. The focal length of the parabolae is given by

$$f=R_0^2/2a, \tag{4}$$

which at the transition to the parabolic-focal-conic texture is approximately $\pi\lambda/2$ or here, about 10 layer thicknesses. Rosenblatt *et al.* [15] predict for a non-ideal layer structure with finite B, that both R_0 and f should increase with increasing dilative stress so that they are proportional to $\sigma^{1/2}$ and σ respectively. Here we have been unable to

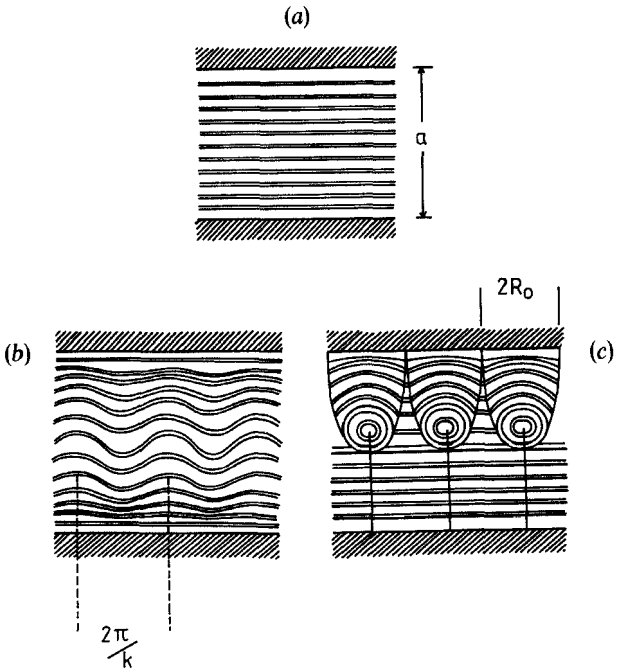

Figure 4. A schematic representation of the effects of subjecting a homeotropic lamellar phase to a dilative stress: (*a*) at low stress $\sigma<\sigma_c$, (*b*) at $\sigma_c<\sigma<1{\cdot}5\sigma_c$, undulations of the lamellae are established and (*c*) at $\sigma>1{\cdot}5\sigma_c$, a parabolic-focal-conic structure is established. The single solid lines represent defects or projections of defects onto the viewing plane. Adapted from [15].

detect any significant changes in R_0, presumably because of its dependence on $\sigma^{1/2}$ and the large distribution in sizes of the parabolic-focal-conic domains (see figure 2). However, the anomalous behaviour manifest in the NMR spectra in figure 1 can now be understood in terms of changes in f. On cooling, the compressional strain arising from the expansion along the normal to the lamellar planes (see figure 5 (*a*)) constrains the lamellae in the homeotropic configuration. On heating, the dilative stress which arises from contraction induces focal domains. The associated director distribution is manifest in a distortion of the NMR spectrum. This increases with temperature due to the increase in σ, and consequently in f.

In contrast, when the experiment is repeated in a solenoid magnet in which the direction of the magnetic field **B** is along the axis of the sample tube such that there are no compressional constraints (figure 5 (*b*)), the spectra obtained (figure 6) show that director distortions now occur also on cooling. This first becomes apparent at 315 K and builds up progressively as the sample is cooled. The spectra, which are found to be invariant for times up to 24 hours, show the build up of a progression of discrete inner doublets which increase in intensity and move inwards (i.e. ϕ increases) as the temperature is lowered. At the lowest temperature, the maxima correspond to director orientations at angles of approximately 10°, 30° and 50°. As the temperature is lowered the lamellae layer spacing increases (see figure 3). This produces a dilatory stress in a direction radial to the axis of the tube and in the plane of the lamellae. There are two possible ways to relax this stress. One is to transport micelles between layers, but this clearly requires compressional stress as in the iron magnet experiment. The other is by way of the formation of edge dislocations (see figure 7), though the alternative possibility of a screw dislocation, or a combination of both [14], cannot be ruled out. The topology of the layers is consistent with there being no directors oriented at

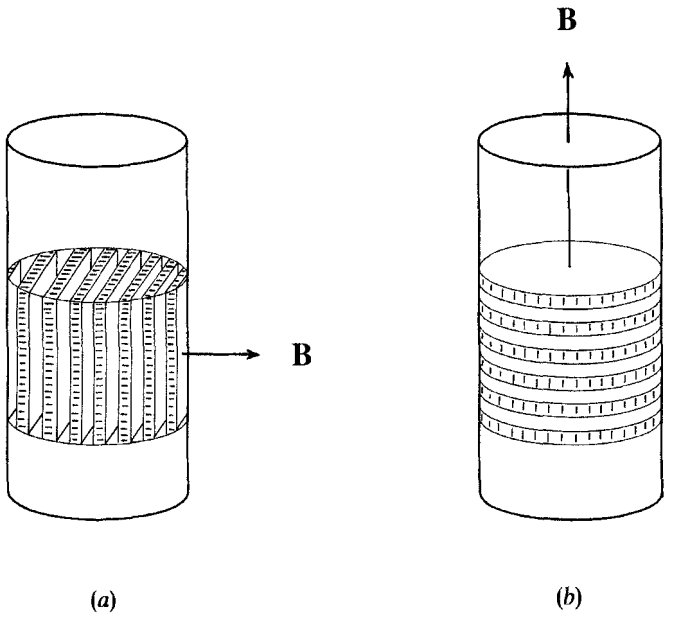

Figure 5. Lamellae constrained (*a*) with the director **n** perpendicular to and (*b*) parallel to the long axis of a cylindrical sample container.

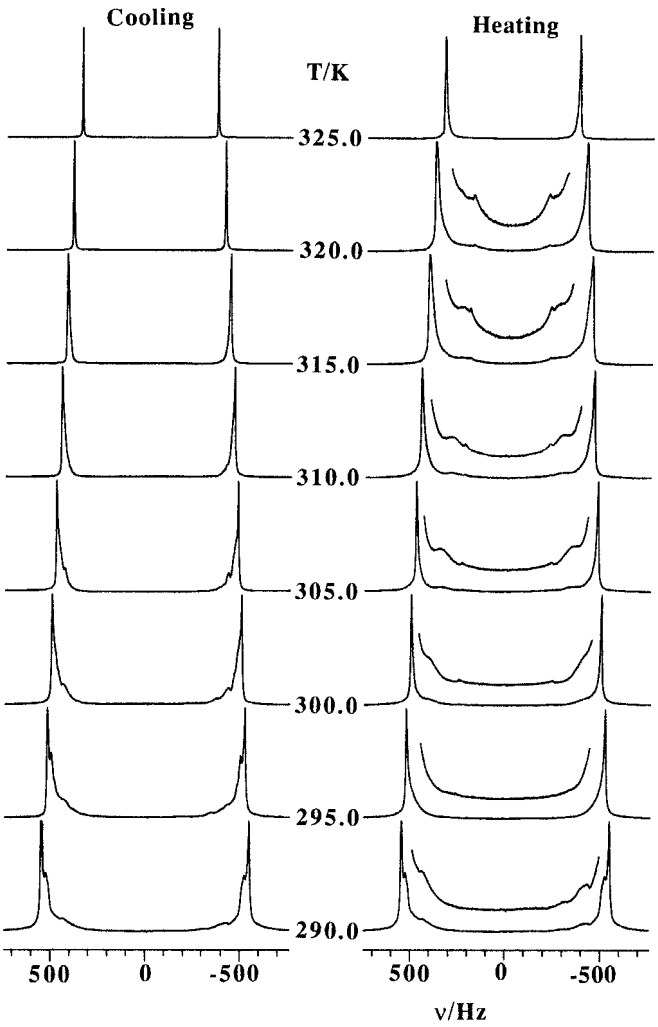

Figure 6. Same as for figure 1 except the spectra were measured at 41·45 MHz using a JEOL GX270 spectrometer with an Oxford Instruments vertical bore solenoid magnet (6·34 T). The long axis of the tube containing the sample is in this case parallel to the direction of the magnetic field.

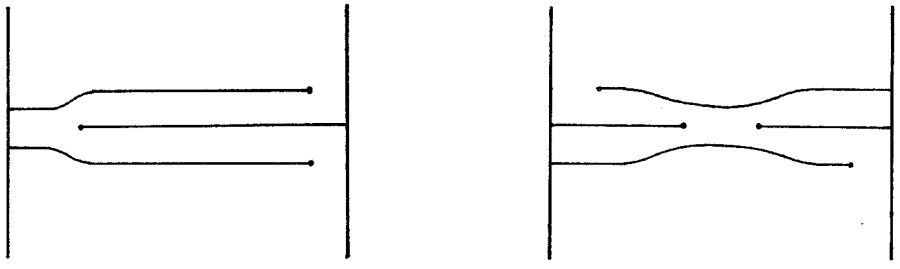

Figure 7. Distortions of lamellae in the vicinity of edge dislocations in the lamellar phase.

$\phi = 90°$. The spectrum obtained on heating from 290 to 295 K shows a more uniform distribution of lamellar directors indicative of the commencement of an annealing process. However, on further heating, singularities occur at one half of the maximum splitting and these increase in intensity with increasing temperature. This is precisely the same behaviour as observed with the iron magnet as can be seen by comparing the spectra at 320 K (see figure 6) and 325 K (see figure 1) and is the result of compressional stress in the plane of the lamellae. The spectrum at 325 K in the solenoid magnet corresponds to a homeotropic lamellar phase. The relaxation of the director distribution in the lamellar phase arises because the sample temperature is now just below that of the lamellar-to-nematic transition ($T_{LN} = 325{\cdot}1$ K). Here, pretransitional fluctuations are becoming significant and the higher magnetic flux density of the solenoid is sufficient to rotate the lamellar directors into uniform alignment along the direction of **B**.

3. Electrical conductivity measurements

These measurements are of interest because they provide information about the diffusivity of the counterions (Cs^+) around the micelles [20]. From this, values can be calculated [5, 21] for the orientational order parameter for the micelles. For macroscopically aligned uniaxial (N_D^+ and L_D) mesophases, the experiment measures the partially averaged component $\tilde{\kappa}_{zz}$ of the conductivity tensor $\boldsymbol{\kappa}$ along the direction of **E** which is taken to be along the z axis of the laboratory frame L(x, y, z). This is given by

$$\tilde{\kappa}_{zz}(\phi) = \kappa_i + 2P_2(\cos\phi)S(\kappa_{\parallel} - \kappa_{\perp})_M/3, \tag{5}$$

where ϕ is the angle between the direction of **E** and the mesophase director **n** which is aligned along the direction of the applied field **B**. κ_i is the trace of $\boldsymbol{\kappa}$ as measured in the isotropic phase ($S = 0$) and in the liquid crystal phases when $\phi = 54°44'$ ($P_2(\cos\phi) = 0$). $(\kappa_{\parallel})_M$ and $(\kappa_{\perp})_M$ are the conductivities measured parallel and perpendicular to the symmetry axes of a static micelle and can be calculated from a knowledge of the micelle dimensions [5]. To obtain values for S, equation (5) is rearranged to give

$$\Delta\tilde{\kappa}/\kappa_i = S(\kappa_{\parallel} - \kappa_{\perp})_M/(\kappa_{\parallel}/3 + 2\kappa_{\perp}/3)_M, \tag{6}$$

where $\Delta\tilde{\kappa} = \tilde{\kappa}_{zz}(0°) - \tilde{\kappa}_{zz}(90°)$. Thus, reliable values for $\tilde{\kappa}_{zz}(0°)$ and $\tilde{\kappa}_{zz}(90°)$ are required. This is not problematical in the N_D^+ phase, but it can be in the L_D phase unless care is taken to ensure there are no distortions of the director in the field. This has been achieved by using the cell illustrated in figure 8, which was designed so as to reproduce the experimental conditions employed in the iron magnet NMR experiments. With this arrangement reliable measurements of $\tilde{\kappa}_{zz}(0°)$ and $\tilde{\kappa}_{zz}(90°)$ are practicable on cooling, but not on heating. Typical behaviour is shown in figure 9. Homeotropic alignment requires equality in the quantities $\tilde{\kappa}_{zz}(54°44')$ and $\{\tilde{\kappa}_{zz}(0°)/3 + 2\tilde{\kappa}_{zz}(90°)/3\}$. This condition is always found to be satisfied on cooling, but not on heating the sample [20], when the values of $\kappa_{zz}(0°)$ and $\tilde{\kappa}_{zz}(90°)$ measured in the L_D phase are seen to deviate towards the κ_i values. This behaviour is consistent with the build up of focal domains on heating the sample.

4. Density measurements

Density measurements are expected to reflect changes in structure, particularly at phase transitions. Thermodynamically, a discontinuity in density is expected at a first order transition whilst, at a second order transition, it should change continuously. The phase transitions in the CsPFO/water system are exceedingly weak [2]. Volume

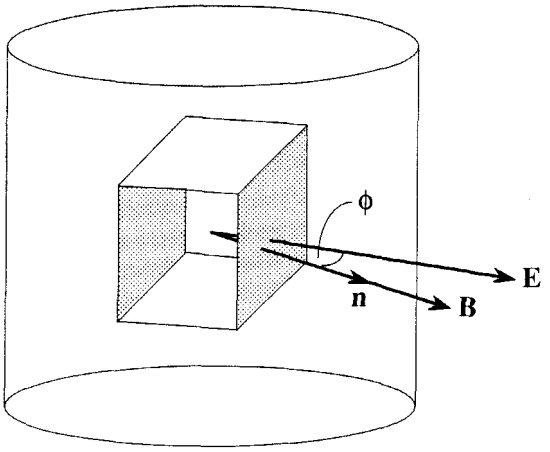

Figure 8. Geometry of the conductivity cell. The sample is contained in a cylindrical cell with an i.d. of 18 mm. The electric field **E** is generated by a pair of platinized platinum 10 mm × 10 mm squares (shaded) placed 10 mm apart. The nematic director is aligned along the direction of the magnetic field **B** (1·0 T) which can be set at any angle ϕ with respect to the direction of **E**. For this cell the orientation of the electric field is not perfectly homogeneous. Taking account of the second rank tensoral property of the conductivity and the distribution of the field orientation, as calculated from a numerical solution to the Laplace equation using the relaxation method, $\tilde{\kappa}_{zz}(0°)$ is calculated to be 7 per cent too high and $\tilde{\kappa}_{zz}(90°)$ 7 per cent too low which leads to a measured anisotropy which is 7 per cent too low.

changes associated with the generation of defects can, therefore, be expected to dominate those associated with the phase transitions unless measurements are made on well oriented monodomains.

The temperature dependence of the specific volume (reciprocal of the density ρ) of a CsPFO/^2H_2O (w = 0·406) sample, as measured using an Anton Paar vibrating-tube digital density meter (Model DMA 60/602), is shown in figure 10. A surprising feature of these results is that both the nematic-to-lamellar and the isotropic-to-nematic transitions are accompanied by a increase rather than the expected decrease in volume. Similar results have been reported [22] for a sample with slightly different concentration (w = 0·409) and have been attributed to changes in the structure of the surfactant aggregates at the phase transitions. These observations are, however, contrary to the findings of Fisch *et al.* [23] that the isotropic-to-nematic transition temperature T_{IN} increases with increasing pressure. Values of T_{IN} were determined for each pressure from the break in slope of the light scattering intensity versus temperature curves as measured in the isotropic phase. Now, as defects will not affect such measurements, it seems expedient to regard them as correctly reflecting the actual volume change at this transition. The pressure dependence of T_{IN} ($dT_{IN}/dp = 2{\cdot}9 \times 10^{-9}$ K Pa^{-1} at 101 kPa for a CsPFO/H_2O (w = 0·406) sample [23]) can be linked to the volume change at the transition by means of the equation $(\partial T_{IN}/\partial p)x_I = T_{IN}\Delta V/\Delta H$, where x_I is the mole fraction of surfactant in the isotropic phase, ΔH is the difference between the enthalpies of the co-existing isotropic and nematic phases, and ΔV is the corresponding difference in the volumes, all at T_{IN}. Taking for ΔH a value -8 J mol^{-1} of surfactant [24], yields a ΔV of only -8×10^{-11} m^3 mol^{-1} which is three orders of

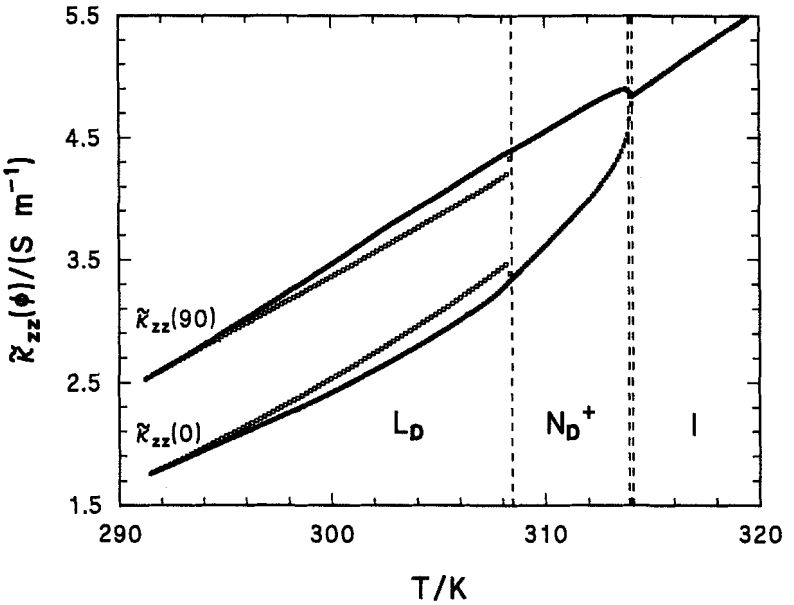

Figure 9. The electrical conductivity $\tilde{\kappa}_{zz}(\phi)$ measured as a function of temperature at 25 kHz for CsPFO/^2H_2O (w = 0·457): T_{IN} = 314·08 K; T_{NI} = 313·90 K; T_{LN} = 308·45 K. The sample was first cooled (closed squares) from the isotropic phase and the conductivity measured at 100 mK intervals allowing 10 min for equilibrium to be attained at each temperature; it was then heated (open squares) from the lamellar phase back to the isotropic phase similarly recording the conductivity.

magnitude smaller than the densitometer value of $+1 \times 10^{-7}\,m^3\,mol^{-1}$ of surfacant. The predicted small change in volume is consistent with the very weak isotropic-to-nematic transition in the CsFPO/water system [2], a consequence of the low packing fraction of the micelles. The only structural change at the transition, apart from the onset of long range orientational order, is an increase of about 15 per cent in the volume of the micelle [5, 25]. Thus, an increase in pressure favours a smaller number of larger discotic micelles: that is, it disfavours high surface curvature, contrary to recent claims that the packing density of amphiphiles is greater in smaller micelles [7, 22].

The ΔV for the nematic-to-isotropic transition must be at least several orders of magnitude smaller than for thermotropics [26]. Such small values seem to be characteristic of phase transitions in amphiphilic systems [27]. Indeed, using a classical dilatometer with a sensitivity of $1 \times 10^{-6}\,cm^3\,g^{-1}$, which is two orders of magnitude less than the volume change at the transition as measured by the densitometer, we were unable to detect any changes in volume or in dV/dT at either transition in a solution of CsPFO/^2H_2O (w = 0·406). Thus, we are led to the conclusion that the large decrease in volume observed at the lamellar-to-nematic and the nematic-to-isotropic transitions in the densitometer experiment must be anomalous. In the densitometer experiments the sample is contained in a U-tube with an internal diameter of only 2 mm, whilst in the dilatometer experiments the sample was contained in a large cylindrical tube of internal diameter 16 mm. Thus the anomalous density changes may be associated in some way or other with defects which are stabilized by their proximity to the surface of the sample container.

To obtain an insight into the nature of the defects which occur in such narrow tubes the optical texture of a sample of CsPFO/^2H_2O (w = 0·535) contained in a glass

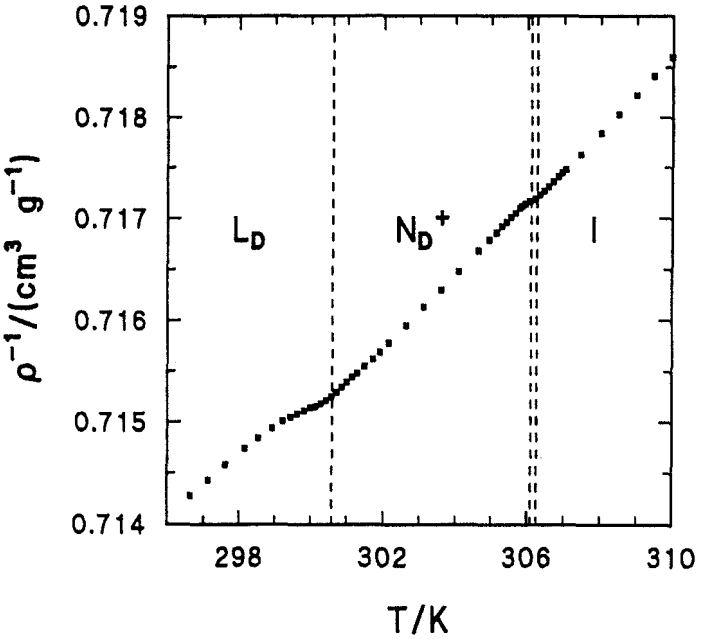

Figure 10. The specific solution volume (density^{-1}) of CsPFO/^2H_2O (w = 0·406), as measured by the Anton Paar vibrating-tube digital density meter (Model DMA 60/602), as a function of temperature: T_{IN} = 306·25 K; T_{NI} = 306·09 K; T_{LN} = 300·60 K. The sample was constrained in a capillary tube with internal diameter of 2 mm. Measurements were taken on cooling from the isotopic phase allowing 10 min for temperature equilibrium to be attained following each temperature change: on heating, the apparent densities reveal hysteresis in the lamellar, but not in the nematic phase [7]. The reproducibility of an individual density measurement in the isotropic phase was better than 3×10^{-6} g cm^{-3}. The temperature of the fluid surrounding the density cell was maintained to $\pm$0·002 K using a Sodev, Model CT-L Circulating Thermostat. The apparent negative volume change associated with both the nematic-to-lamellar and the isotropic-to-nematic transitions is clearly seen.

capillary with a 1 mm internal diameter was studied on cooling/heating across the phase transitions. A 1 mm internal diameter sample tube was chosen so as to minimize the problems arising from depth of focus problems for tubes with a cylindrical cross section. Figure 11 (*a*) shows the Schlieren texture observed a few minutes after cooling into the nematic phase at 325·7 K (1·3 K below T_{NI}) at a cooling rate of 2 K/min. Figure 11 (*b*) shows the same region after further cooling to 323·3 K, the small domains separated by a large number of defects have gone and the domains are large with few macroscopic defects. Cooling slowly into the lamellar phase to just below the transition, shows an almost unchanged domain structure, though the texture changes to that of a lamellar phase. Further cooling, at a rate of 2 K/min, is accompanied by surface ordering of the lamellae by the walls of the container, as indicated by the smooth birefringent texture in the vicinity of the walls, and the appearance of a central axial defect-line of disclinations (see figure 11 (*c*)). The defect develops with time and after two weeks at room temperature in a sealed tube is very well defined (see figure 11 (*d*)). Raising the temperature by 5 K causes the surface induced order to break up as a consequence of a dilatory stress arising from the contraction of the bilayers (see figure 11 (*e*)).

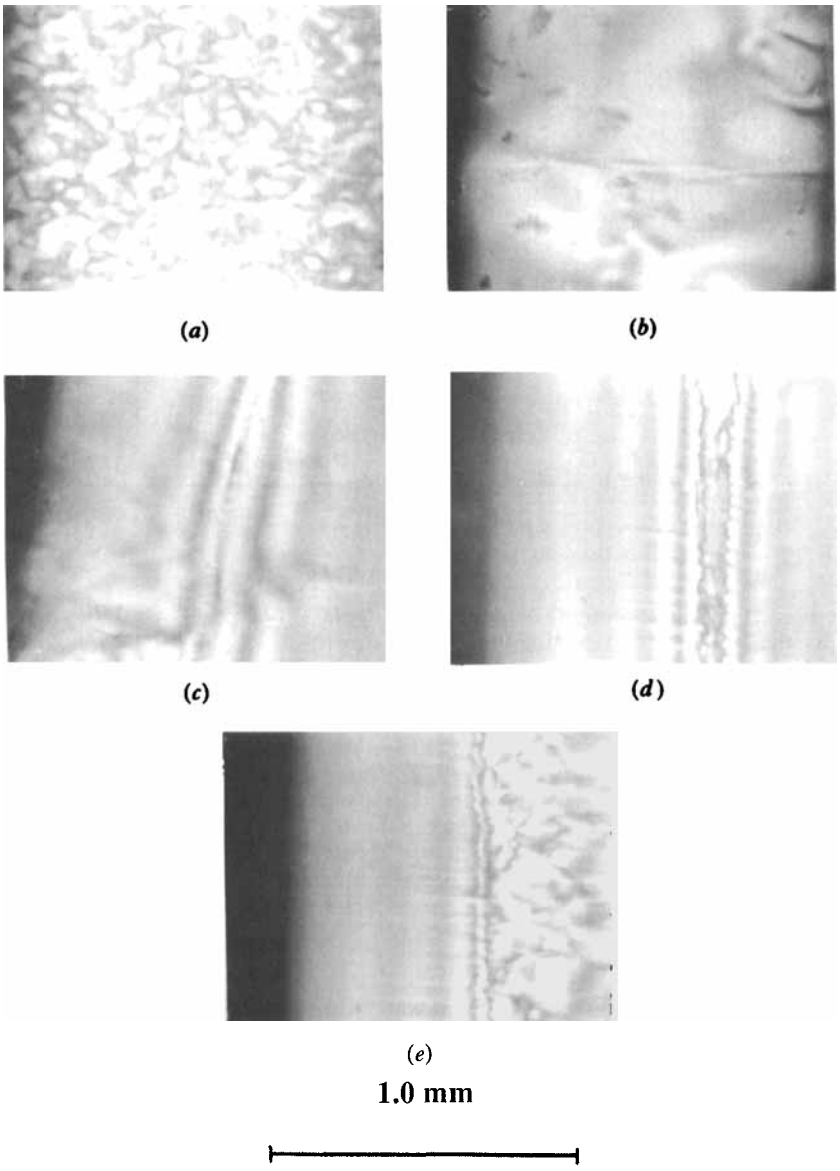

Figure 11. Photomicrographs of CsPFO/^2H_2O (w = 0·535) contained in a glass capillary of internal diameter of 1 mm: T_{IN} = 327·5 K; T_{NI} = 327·0 K; T_{NL} = 322·4 K; T_{LN} = 322·0 K. (*a*) A few minutes after cooling into the nematic phase (325·7 K) at a cooling rate of 2 K/min. The Schlieren texture indicates small nematic domains separated by a large number of defects. (*b*) The same region after cooling to 323·3 K. The defects have been largely annealed out, the nematic domains are large and there are few macroscopic defects. (*c*) After cooling to 310·2 K in the lamellar phase, a central axial defect is beginning to develop. (*d*) Appearance of the axial defect after leaving the sample in a sealed tube at room temperature ($\approx$ 294 K) for two weeks. The axial defect is now well developed. (*e*) Appearance of the same region shown in (*d*) immediately after heating the lamellar sample to 299·0 K. Dilatory stress causes a break-up in the surface induced ordering. This can be seen on the right of the central axial defect. The pattern is asymmetric as a result of the poor thermal contact between the cylindrical sample tube and the flat hot stage.

Clearly, the macroscopic density as measured in the densitometer experiments would be subject to any of the changes in macroscopic defect structure shown here. However, the associated volume changes are not expected to be of the same order of magnitude as those observed. Indeed, if they were, they would also be apparent in the dilatometer measurements. An alternative explanation is that the ordered phases are churned-up in some way which is dependent upon their viscosity/elastic properties which, in turn, are determined by their long-range structural organization, i.e. the vibration of the densitometer sample tube is driving the system into complex non-equilibrium configurations.

5. Conclusions

It has been demonstrated that a variety of defects can occur in monodomain nematic (disclinations) and lamellar (disclinations, dislocations, and focal domains) phases of the CsPFO/water system, in a manner dependent on the constraints imposed by the sample container and thermal history. Other lyotropic liquid crystals can be expected to behave similarly. The presence of these defects can, as we have show, give rise to anomalous effects in experiments. Cognizance of the conditions that lead to the generation of particular defects may, in appropriate cases, enable them to be avoided.

We wish to thank the Science and Engineering Research Council for project grants to N.B., a studentship to D.P. and a visiting fellowship for K.W.J. We also thank the Royal Society of London and the British Council for travel grants to N.B. and K.W.J., respectively, and the University Grants Committee for an equipment grant to K.W.J.

References

[1] Boden, N., Jackson, P. H., McMullen, K., and Holmes, M. C., 1979, *Chem. Phys. Lett.*, **65**, 476.
[2] Boden, N., Corne, S. A., and Jolley, K. W., 1987, *J. phys. Chem.*, **91**, 4092.
[3] Boden, N., Jolley, K. W., and Smith, M. H., 1989, *Liq. Crystals*, **6**, 481.
[4] Boden, N., and Holmes, M. C., 1984, *Chem. Phys. Lett.*, **109**, 76.
[5] Boden, N., Corne, S. A., Holmes, M. C., Jackson, P. H., Parker, D., and Jolley, K. W., 1986, *J. Phys., Paris*, **47**, 2135.
[6] Holmes, M. C., Reynolds, D. J., and Boden, N., 1987, *J. phys. Chem.*, **91**, 5257.
[7] Photinos, P., and Saupe, A., 1990, *Phys. Rev.* A, **41**, 954.
[8] Fontell, K., and Lindman, B., 1983, *J. phys. Chem.*, **87**, 3289.
[9] Reizlein, K., and Hoffman, H., 1984, *Prog. Colloid Polymer Sci.*, **69**, 83.
[10] Hoffman, H., 1984, *Ber. Bunsenges phys. Chem.*, **88**, 1078.
[11] Herbst, L., Hoffman, H., Kalus, J., Reizlein, K., Schmelzer, U., and Ibel, K., 1985, *Ber. Bunsenges phys. Chem.*, **89**, 1050.
[12] Photinos, P., and Saupe, A., 1986, *J. chem. Phys.*, **84**, 517.
[13] Photinos, P., and Saupe, A., 1986, *J. chem. Phys.*, **85**, 7467.
[14] Kléman, M., 1989, *Rep. Prog. Phys.*, **52**, 555.
[15] Rosenblatt, C. S., Pindak, R., Clark, N. A., and Meyer, R. B., 1977, *J. Phys., Paris*, **38**, 1105.
[16] Benton, W. J., Toor, E. W., Miller, C. A., and Fort, T. Jr., 1979, *J. Phys., Paris*, **40**, 107.
[17] Asher, S. A., and Pershan, P. S., 1979, *J. Phys., Paris*, **40**, 161.
[18] Clark, N., and Meyer, R. B., 1973, *Appl. Phys. Lett.*, **22**, 493.
[19] Delaye, M., Ribotta, R., and Durand, G., 1973, *Physics Lett.* A, **44**, 139.
[20] Boden, N., Corne, S. A., and Jolley, K. W., 1984, *Chem. Phys. Lett.*, **105**, 99.
[21] Boden, N., Parker, D., and Jolley, K. W., 1987, *Molec. Crystals liq. Crystals*, **152**, 121.
[22] Photinos, P., and Saupe, A., 1989, *J. chem. Phys.*, **90**, 5011.

[23] FISCH, M. R., KUMAR, S., and LITSTER, J. D., 1986, *Phys. Rev. Lett.*, **57**, 2830.
[24] CHIN, S. T., and KUMAR, S., 1991, *Phys. Rev. Lett.*, **66**, 1062.
[25] BODEN, N., CLEMENTS, J., JOLLEY, K. W., PARKER, D., and SMITH, M. H., 1990, *J. chem. Phys.*, **93**, 9096.
[26] TORZA, S., and CLADIS, P. E., 1974, *Phys. Rev. Lett.*, **32**, 1406. RAO, N. V. S., and PISIPATI, V. G. K. M., 1983, *J. phys. Chem.*, **87**, 899. GUICHARD, Y., SIGAUD, G., and HARDOUIN, F., 1984, *Molec. Crystals liq. Crystals*, **102**, 325.
[27] CLUNIE, J. S., GOODMAN, J. F., and SYMONS, P. C., 1969, *Trans. Faraday Soc.*, **65**, 287.